CU-TP/99-01

Atmospheric Neutrino Oscillations in Three-Flavor Neutrinos. II

Toyokazu SAKAI and Tadayuki TESHIMA*)

Department of Applied Physics, Chubu University, Kasugai 487-8501, Japan

We analyze the atmospheric neutrino experiments of SuperKamiokande (535 days) using the three-flavor neutrino framework with the mass hierarchy $m_1 \approx m_2 \ll m_3$. We study the event ratios of sub-GeV, multi-GeV and upward through-going muons zenith angle distributions. Taking into account the atmospheric and terrestrial experiments, we obtain the allowed regions of mass and mixing parameters Δm^2_{12}, $\sin^2 2\theta_{12}$, Δm^2_{23}, θ_{13} and θ_{23}. The mass parameter Δm^2_{23} is restricted to $0.01\,\mathrm{eV}^2$-$0.0002\,\mathrm{eV}^2$. For mixing parameters, there is no difference between the large θ_{12} angle solution and the small one, and $\theta_{13} < 13^\circ$, $28^\circ < \theta_{23} < 37^\circ$ and $53^\circ < \theta_{23} < 62^\circ$ for $\Delta m^2_{23} = 0.01\,\mathrm{eV}^2$, $\theta_{13} < 23^\circ$ and $29^\circ < \theta_{23} < 61^\circ$ for $\Delta m^2_{23} = 0.002\,\mathrm{eV}^2$, $4^\circ < \theta_{13} < 22^\circ$ and $38^\circ < \theta_{23} < 54^\circ$ for $\Delta m^2_{23} = 0.0002\,\mathrm{eV}^2$.

§1. Introduction

SuperKamiokande experiment [1] has observed a definite atmospheric neutrino anomaly and confirmed a hypothesis of neutrino oscillation. In their two-flavor mixing analyses of the sub-GeV and multi-GeV zenith angle distribution, it has been obtained that the $\nu_\mu \leftrightarrow \nu_\tau$ oscillation is preferred over the $\nu_\mu \leftrightarrow \nu_e$ oscillation and the range of mass parameter Δm^2 is from $3 \times 10^{-4}\mathrm{eV}^2$ to $0.8 \times 10^{-2}\mathrm{eV}^2$. [1]

Observing the neutrino oscillations is one of the most important experiments suggesting a new physics beyond the standard model. Constructing a model beyond the standard model, it is necessary to confirm the mixing and mass parameters of three neutrinos in the low energy region although there is no restriction on number of neutrinos in very high energy region. [2] The three-flavor neutrinos scenario [3] is found to be consistent with above the large $\nu_\mu \leftrightarrow \nu_\tau$ oscillation and the solar neutrino anomaly [4] and terrestrial neutrino experiments. [5),6),7)] K2K, MINOS and CERN-Gran Sasso long-baseline experiments [8] are in preparation to confirm the $\nu_\mu \leftrightarrow \nu_e$ and $\nu_\mu \leftrightarrow \nu_\tau$ oscillation precisely. Then it becomes important to examine the mass and mixing parameters in the three-flavor neutrinos framework [3),9)] precisely.

In this paper, we analyze the SuperKamiokande atmospheric neutrino experiment (535 days) of the sub-GeV, multi-GeV and upward through-going muons zenith angle distributions in the three-flavor neutrino framework with a hierarchy of neutrino masses $m_1 \approx m_2 \ll m_3$. In a previous work, [10] we have analyzed the zenith angle distributions in the

*) E-mail: teshima@isc.chubu.ac.jp

SuperKamiokande atmospheric neutrino experiment(325.8 days).[11] In that work, we analyzed the double ratios of the sub-GeV and multi-GeV zenith angle distributions neglecting the matter effects of the Earth and the difference between incident neutrinos and detected charged leptons.

In the three-flavor neutrino framework with the hierarchy $m_1 \approx m_2 \ll m_3$, there are 5 parameters $\theta_{12},\ \theta_{13},\ \theta_{23},\ \Delta m^2_{12} = m^2_2 - m^2_1,\ \Delta m^2_{23} = m^2_3 - m^2_2$ concerned with the neutrino oscillation. For solar neutrino deficit, the MSW solution[12),13),10)] taking into account the matter effects predicts the large angle solution $\sin^2 2\theta_{12} = 0.6$–$0.9,\ \Delta m^2_{12} = 4 \times 10^{-6}$–$7 \times 10^{-5}\mathrm{eV}^2$ and small angle solution $\sin^2 2\theta_{12} = 0.003$–$0.01,\ \Delta m^2_{12} = 3 \times 10^{-6}$–$1.2 \times 10^{-5}\mathrm{eV}^2$ for $\theta_{13} = 0°$–$20°$, and these large and small angle solution are merged for $\theta_{13} = 25°$–$50°$. The vacuum solution for solar neutrinos is obtained as $\Delta m^2_{12} \sim 10^{-10}\mathrm{eV}^2$.[14] In terrestrial neutrino experiments, Fogli *et al.*[15] have thoroughly analyzed and obtained the allowed regions in $\tan^2\theta_{13}$–$\tan^2\theta_{23}$ plane for various values of the mass parameter Δm^2_{23}. We also analyzed the terrestrial neutrino experiments,[10] and obtained results similar to those of Fogli et al. The allowed region in $\tan^2\theta_{13} - \tan^2\theta_{23}$ plane was more restricted for higher values of Δm^2_{23}, and the allowed region spread out for lower values of it. In this paper, we combine the results obtained from the atmospheric neutrino experiments of SuperKamiokande and the terrestrial experiments to obtain the allowed regions for mixing and mass parameters in three-flavor neutrinos.

§2. Neutrino oscillation in three-flavor neutrinos

The unitary matrix U representing the neutrino mixing is defined as

$$\nu_{l_\alpha} = \sum_{\beta=1}^{3} U_{l_\alpha\beta}\nu_\beta, \quad l_\alpha = e,\ \mu, \tau, \tag{1}$$

where the states ν_{l_α} and ν_β are the flavor and mass eigenstate of neutrinos, respectively. This mixing matrix corresponds to the CKM matrix $U^\dagger_{\mathrm{CKM}}$ for quarks sector. We parameterize the unitary matrix neglecting the *CP* violation phases as

$$\begin{aligned} U &= \exp(i\theta_{23}\lambda_7)\exp(i\theta_{13}\lambda_5)\exp(i\theta_{12}\lambda_2) \\ &= \begin{pmatrix} c^\nu_{12}c^\nu_{13} & s^\nu_{12}c^\nu_{13} & s^\nu_{13} \\ -s^\nu_{12}c^\nu_{23} - c^\nu_{12}s^\nu_{23}s^\nu_{13} & c^\nu_{12}c^\nu_{23} - s^\nu_{12}s^\nu_{23}s^\nu_{13} & s^\nu_{23}c^\nu_{13} \\ s^\nu_{12}s^\nu_{23} - c^\nu_{12}c^\nu_{23}s^\nu_{13} & -c^\nu_{12}s^\nu_{23} - s^\nu_{12}c^\nu_{23}s^\nu_{13} & c^\nu_{23}c^\nu_{13} \end{pmatrix}, \\ & \qquad c^\nu_{ij} = \cos\theta^\nu_{ij}, \quad s^\nu_{ij} = \sin\theta^\nu_{ij}, \end{aligned} \tag{2}$$

where the λ_i are the Gell-Mann matrices.

The probabilities for transitions $\nu_{l_\alpha} \to \nu_{l_\beta}$ are written as

$$P(\nu_{l_\alpha} \to \nu_{l_\beta}) = |<\nu_{l_\beta}(t)|\nu_{l_\alpha}(0)>|^2 = \delta_{l_\alpha l_\beta} + p^{12}_{\nu_{l_\alpha}\to\nu_{l_\beta}} S_{12}$$

$$
\begin{aligned}
&+p^{23}_{\nu_{l_\alpha}\to\nu_{l_\beta}}S_{23}+p^{31}_{\nu_{l_\alpha}\to\nu_{l_\beta}}S_{31},\\
p^{12}_{\nu_{l_\alpha}\to\nu_{l_\beta}}&=-2\delta_{l_\alpha l_\beta}(1-2U^2_{l_\alpha 3})+2(U^2_{l_\alpha 1}U^2_{l_\beta 1}+U^2_{l_\alpha 2}U^2_{l_\beta 2}-U^2_{l_\alpha 3}U^2_{l_\beta 3}),\\
p^{23}_{\nu_{l_\alpha}\to\nu_{l_\beta}}&=-2\delta_{l_\alpha l_\beta}(1-2U^2_{l_\alpha 1})+2(-U^2_{l_\alpha 1}U^2_{l_\beta 1}+U^2_{l_\alpha 2}U^2_{l_\beta 2}+U^2_{l_\alpha 3}U^2_{l_\beta 3}),\\
p^{31}_{\nu_{l_\alpha}\to\nu_{l_\beta}}&=-2\delta_{l_\alpha l_\beta}(1-2U^2_{l_\alpha 2})+2(U^2_{l_\alpha 1}U^2_{l_\beta 1}-U^2_{l_\alpha 2}U^2_{l_\beta 2}+U^2_{l_\alpha 3}U^2_{l_\beta 3}),
\end{aligned}
\tag{3}
$$

where S_{ij} is the term representing the neutrino oscillation;

$$
S_{ij}=\sin^2 1.27\frac{\Delta m^2_{ij}}{E}L. \tag{4}
$$

Here $\Delta m^2_{ij}=|m^2_i-m^2_j|$, E and L are measured in units eV^2, GeV and km, respectively.

The values of neutrino masses are not known precisely, but two mass parameters are necessary to account for the solar neutrino experiments and the atmospheric neutrino experiments. In the former, mass parameter Δm^2 is obtained as 10^{-4}–$10^{-5}\,\mathrm{eV}^2$ [4), 13), 10)] or $\sim 10^{-10}\mathrm{eV}^2$, [14)] and in the latter, Δm^2 is obtained as $10^{-1}-10^{-3}\mathrm{eV}^2$. [11), 16)] Then it seems that the most reasonable mass hierarchy is that in which the lower two neutrino masses of three neutrinos are very close and the third is rather far from them. Thus we assume that three neutrino masses have a mass hierarchy obeying

$$
m_1\approx m_2\ll m_3. \tag{5}
$$

With the hierarchy Eq. (5), $\Delta m^2_{12}\ll\Delta m^2_{23}\simeq\Delta m^2_{13}$, Eq. (3) for the transition probabilities $P(\nu_{l_\alpha}\to\nu_{l_\beta})$ can be rewritten as

$$
\begin{aligned}
P(\nu_{l_\alpha}\to\nu_{l_\alpha})&=1-2(1-2U^2_{l_\alpha 3}-U^4_{l_\alpha 1}-U^4_{l_\alpha 2}+U^4_{l_\alpha 3})S_{12}-4U^2_{l_\alpha 3}(1-U^2_{l_\alpha 3})S_{23},\\
P(\nu_{l_\alpha}\to\nu_{l_\beta})&=P(\nu_{l_\beta}\to\nu_{l_\alpha})=2(U^2_{l_\alpha 1}U^2_{l_\beta 1}+U^2_{l_\alpha 2}U^2_{l_\beta 2}-U^2_{l_\alpha 3}U^2_{l_\beta 3})S_{12}\\
&\quad+4U^2_{l_\alpha 3}U^2_{l_\beta 3}S_{23}.
\end{aligned}
\tag{6}
$$

In the atmospheric neutrino experiments, especially in the sub-GeV ones, the matters of the Earth have the important effects. Matter effects are induced by the quantity $A=2\sqrt{2}EG_FN_e$. In the Earth, $N_e\sim 3\mathrm{mol/cm}^3$, thus $A\sin 2\theta_{13}<<1$ and we can approximate the mixing matrix U as [12)]

$$
U^M=\exp(i\lambda_7\theta_{23})\exp(i\lambda_5\theta_{13})\exp(i\lambda_2\theta^M_{12}), \tag{7}
$$

where

$$
\begin{aligned}
&\sin 2\theta^M_{12}=\tfrac{\Delta m^2_{12}}{\Delta m^{M2}_{12}}\sin 2\theta_{12},\\
&\Delta m^{M2}_{12}=m^{M2}_2-m^{M2}_1,\quad \Sigma=m^2_1+m^2_2,\\
&m^{M2}_{1,2}=\tfrac{1}{2}\left\{(\Sigma+A\cos^2\theta_{13})\mp\sqrt{(A\cos^2\theta_{13}-\Delta m^2_{12}\cos 2\theta_{12})^2+(\Delta m^2_{12}\sin 2\theta_{12})^2}\right\},\\
&m^{M2}_3=m^2_3+A\sin^2\theta_{13}.
\end{aligned}
$$

This expression corresponds to the neutrino case, and A enters in this expression with opposite sign for the anti-neutrino case. If we approximate the density of the Earth to be uniform, we can take the expressions for the transition probability with matter effects as

$$\begin{aligned} P^M(\nu_{l_\alpha} \to \nu_{l_\alpha}) &= 1 - 2(1 - 2U_{l_\alpha 3}^{M2} - U_{l_\alpha 1}^{M4} - U_{l_\alpha 2}^{M4} + U_{l_\alpha 3}^{M4})S_{12}^M - 4U_{l_\alpha 3}^{M2}(1 - U_{l_\alpha 3}^{M2})S_{23}^M, \\ P^M(\nu_{l_\alpha} \to \nu_{l_\beta}) &= P^M(\nu_\beta \to \nu_\alpha) = 2(U_{l_\alpha 1}^{M2}U_{l_\beta 1}^{M2} + U_{l_\alpha 2}^{M2}U_{l_\beta 2}^{M2} - U_{l_\alpha 3}^{M2}U_{l_\beta 3}^{M2})S_{12}^M \\ &\quad + 4U_{l_\alpha 3}^{M2}U_{l_\beta 3}^{M2}S_{23}^M, \end{aligned} \tag{8}$$

where

$$S_{ij}^M = \sin^2 1.27\frac{\Delta m_{ij}^{M2}}{E}L. \tag{9}$$

§3. Numerical analyses of neutrino oscillations

3.1. *Atmospheric neutrinos*

Evidence for an anomaly in atmospheric neutrino experiments was pointed out in reports of Kamiokande collaboration [17),18)] and IMB collaboration [19)] using water-Cherencov experiments. More recently, reports of SuperKamiokande collaboration [11),1)] have provided more precise results on the anomaly in atmospheric neutrinos. In our previous papers, [10)] we have analyzed the double ratios $R(\mu/e) \equiv R_{\rm expt}(\mu/e)/R_{\rm MC}(\mu/e)$ of atmospheric neutrinos. In this work, we analyze the event ratio $N_{\rm Exp}(l_\alpha)/N_{\rm MC}(l_\alpha)$, where l_α represents μ and e.

The zenith angle distributions of sub-GeV, multi-GeV events and upward through-going μ fluxes are taken from the SuperKamiokande 535 days experiments. [1)] The data are tabulated in Table I. These values are taken from the experimental event data and Monte-Carlo simulations which are given graphically in Ref. 1). μ-like events include the fully contained and partially contained events. Errors represent statistical ones only. In the above data, sub-GeV experiments detect the visible-energy less than 1.33GeV.

The zenith angle θ dependent events $dN_{\rm Exp}(l_\alpha)/d\cos\theta$ and $dN_{\rm MC}(l_\alpha)/d\cos\theta$ are defined as

$$\frac{dN_{\rm Exp}(l_\alpha)}{d\cos\theta} = \sum_\beta \int \epsilon_\alpha(E_\alpha)\sigma_\alpha(E_\nu, E_\alpha, \psi)F_\beta(E_\nu, \theta - \psi)P^M(\nu_\beta \to \nu_\alpha)dE_\alpha dE_\nu d\cos\psi, \tag{10a}$$

$$\frac{dN_{\rm MC}(l_\alpha)}{d\cos\theta} = \int \epsilon_\alpha(E_\alpha)\sigma_\alpha(E_\nu, E_\alpha, \psi)F_\alpha(E_\nu, \theta - \psi)dE_\alpha dE_\nu d\cos\psi, \tag{10b}$$

where the summation $\sum_\beta$ are taken over ν_μ and ν_e. In these expressions, processes of $\bar{\nu}_\mu$ and$\bar{\nu}_e$ are contained. $\epsilon_\alpha(E_\alpha)$ is the detection efficiency of the detector for α-type charged lepton with energy E_α. $\sigma_\alpha(E_\nu, E_\alpha, \psi)$ is the differential cross section of scattering l_α with energy E_ν by incident ν_α with energy E_α, where angle ψ is the scattering angle relative to the direction of incident ν_α. $F_\beta(E_\nu, \theta)$ is the incident ν_β flux with energy E_ν at the zenith angle θ. $P^M(\nu_\alpha \to \nu_\beta)$ is the transition probability with the matter effects expressed in

Table I. e-like, μ-like atmospheric neutrino data and upward through-going muons fluxes of SuperKamiokande experiments (535days data). These values are the ratios of experimental data and Monte-Carlo simulations which are obtained from the graphs in Ref. 1). μ-like events include fully contained and partially contained events, and errors represent statistical ones only.

Sub-GeV data

$\cos\theta$ range	e-like event ratio $N_{\rm Exp}/N_{\rm MC}$	μ-like event ratio $N_{\rm Exp}/N_{\rm MC}$
-1.0 − -0.6	1.37 ± 0.09	0.56 ± 0.04
-0.6 − -0.2	1.12 ± 0.08	0.71 ± 0.05
-0.2 − 0.2	1.18 ± 0.08	0.74 ± 0.05
0.2 − 0.6	1.05 ± 0.08	0.86 ± 0.06
0.6 − 1.0	1.15 ± 0.08	0.82 ± 0.05

Multi-GeV data

$\cos\theta$ range	e-like event ratio $N_{\rm Exp}/N_{\rm MC}$	μ-like event ratio $N_{\rm Exp}/N_{\rm MC}$
-1.0 − -0.6	1.35 ± 0.21	0.56 ± 0.07
-0.6 − -0.2	1.10 ± 0.16	0.57 ± 0.07
-0.2 − 0.2	1.13 ± 0.15	0.79 ± 0.07
0.2 − 0.6	1.42 ± 0.18	1.02 ± 0.09
0.6 − 1.0	1.18 ± 0.20	1.03 ± 0.10

Upward through-going μ data

$\cos\theta$ range	μ flux ratio $N_{\rm Exp}/N_{\rm MC}$
-1.0 − -0.9	0.77 ± 0.14
-0.9 − -0.8	0.79 ± 0.12
-0.8 − -0.7	0.58 ± 0.11
-0.7 − -0.6	0.96 ± 0.13
-0.6 − -0.5	0.73 ± 0.10
-0.5 − -0.4	0.80 ± 0.10
-0.4 − -0.3	0.74 ± 0.10
-0.3 − -0.2	0.92 ± 0.10
-0.2 − -0.1	1.02 ± 0.10
-0.1 − 0.0	1.09 ± 0.10

Eq. (8) and it depends on the energy E_ν and the distance L. This distance depends on the zenith angle θ as $L = \sqrt{(r+h)^2 - r^2 \sin^2\theta} - r\cos\theta$, where r is the radius of the Earth and h is the altitude of the production point of atmospheric neutrinos.

Informations of $F_\beta(E_\nu, \theta)$ for multi-GeV case are given in Refs. 20),21),23). Informations of $F_\beta(E_\nu, \theta)$ including the geomagnetic effects for sub-GeV case are taken from Ref. 22). Other informations of $\epsilon_\alpha(E_\alpha)$ and $\sigma_\alpha(E_\nu, E_\alpha, \psi)$ are given in Ref. 24). The upward through-going muons fluxes are simulated in Ref. 24). Explicit calculation of Eq. (10) is explained in Appendix A.

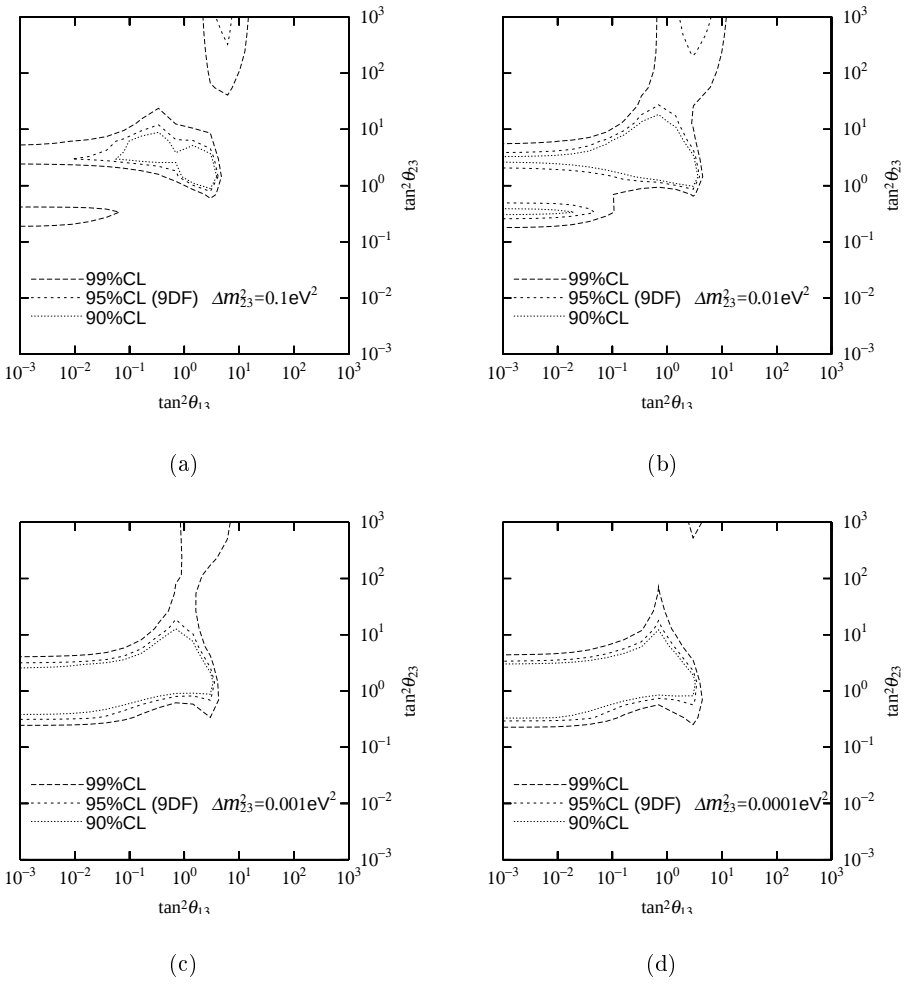

Fig. 1. The plots of allowed regions in the $\tan^2\theta_{13}$–$\tan^2\theta_{23}$ plane determined by the zenith angle distributions of SuperKamiokande 535 days data. These figures correspond to the large θ_{12} angle solution, $\Delta m^2_{12} = 3\times10^{-5}\mathrm{eV}^2$ and $\sin^2 2\theta = 0.7$. In these figures, broken thick, broken thin and dotted curves denote the regions allowed in 99%, 95% and 90% C.L., respectively. Figs. (a)–(d) show the plots of sub-GeV experiments.

Since $P^M(\nu_\alpha \to \nu_\beta)$ is the function of $\Delta m^2_{12}, \Delta m^2_{23}, \theta_{12}, \theta_{13}$ and θ_{23}, the ratio $(dN_{\mathrm{Exp}}(l_\alpha)/d\cos\theta)/(dN_{\mathrm{MC}}(l_\alpha)/d\cos\theta)$ of the zenith angle distributions is a function of $\Delta m^2_{12}, \Delta m^2_{23}, \theta_{12}, \theta_{13}, \theta_{23}$ and θ. We analyze the atmospheric neutrino data fixing the parameters Δm^2_{12}

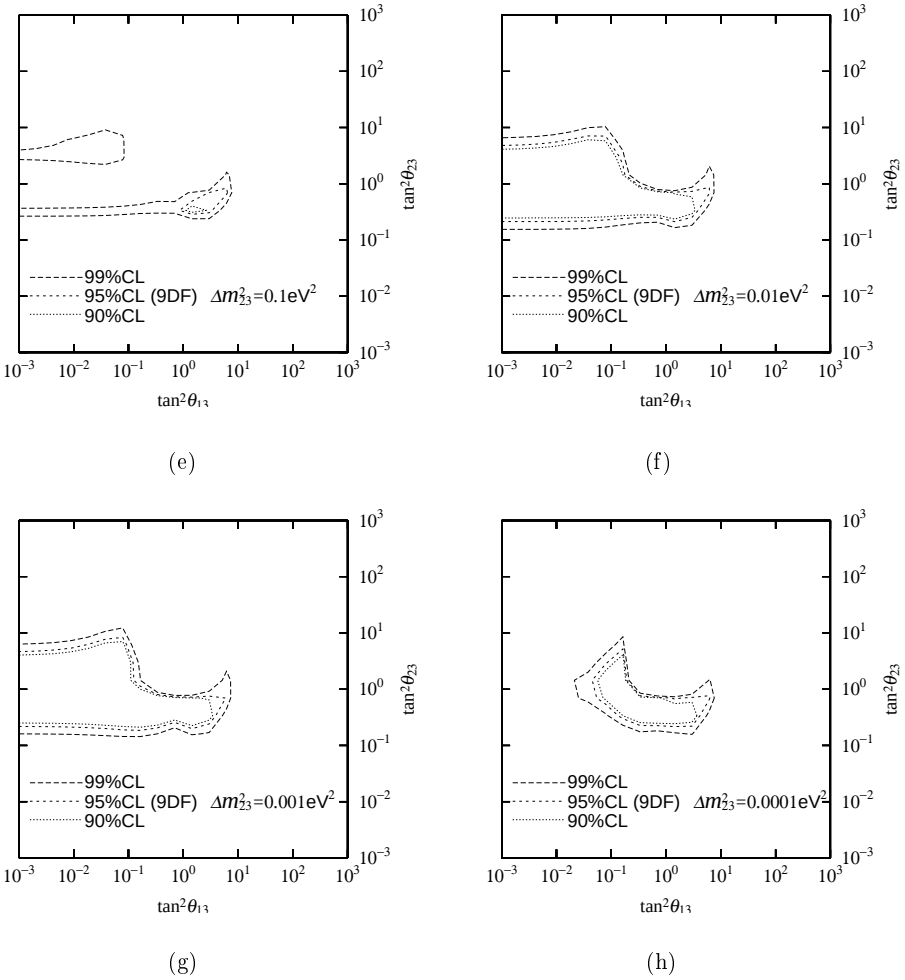

Fig. 1. The plots of allowed regions in the $\tan^2\theta_{13}$–$\tan^2\theta_{23}$ plane. Figs. (e)–(h) the plots of multi-GeV experiments.

and $\sin^2 2\theta_{12}$, which have been determined from the solar neutrino experiments,[4),13),10)] as $\Delta m^2_{12} = 3\times10^{-5}\mathrm{eV}^2$ and $\sin^2 2\theta_{12} = 0.7$, which corresponds to the large angle solution, and $\Delta m^2_{12} = 10^{-5}\mathrm{eV}^2$ and $\sin^2 2\theta_{12} = 0.005$, which corresponds to the small angle solution. We treat the ratios of the zenith angle distributions of the experimental events and the ones of Monte-Calro simulation, $(N_{\mathrm{Exp}}(l_\alpha)/N_{\mathrm{MC}}(l_\alpha))_i$, where i represents the region number of the bins of zenith angle θ.

We treat the χ^2 defined as

$$\chi^2 = \sum_{i,\ l_\alpha} \frac{\left\{(N_{\mathrm{Exp}}(l_\alpha)/N_{\mathrm{MC}}(l_\alpha))_i^{\mathrm{cal}} - (N_{\mathrm{Exp}}(l_\alpha)/N_{\mathrm{MC}}(l_\alpha))_i^{\mathrm{data}}\right\}^2}{(\sigma_{st})_i^2 + (\sigma_{sy})_i^2}. \tag{11}$$

For the sub-GeV and multi-GeV experiments, the summation on i are over 1 to 5 of zenith angle range bins and for the upward through-going μ, 1 to 10. The summation on l_α are over μ and e for the sub-GeV and multi-GeV experiments. We estimate the χ^2 on the

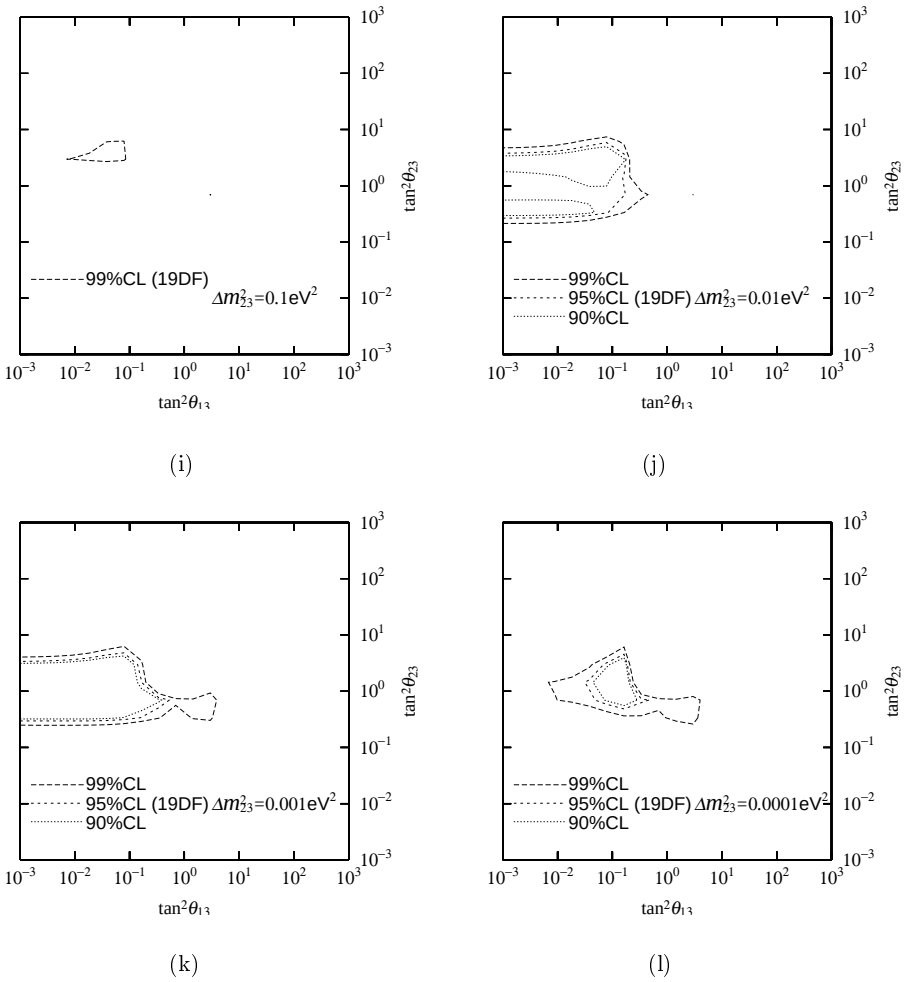

Fig. 1. The plots of allowed regions in the $\tan^2\theta_{13}$–$\tan^2\theta_{23}$ plane. Figs. (i)–(l) show the plots of the combinations of the sub-GeV and multi-GeV experiments.

various of $\Delta m^2_{23}, \theta_{13}$ and θ_{23}. σ_{st} represents the statistical error and σ_{sy} systematic one. We adopt the values of σ_{sy} which are induced from the magnitudes of 10% of the $N_{\rm MC}$ assumed as uncertainty. These values are deduced from the graphs given by the report of SuperKamiokande collaboration.[1)] In Fig. 1, we showed the contour plots of χ^2 in the $\tan^2\theta_{13}$–$\tan^2\theta_{23}$ plane for various Δm^2_{23}. We showed the plots of sub-GeV experiment in Fig. 1(a)–(d) and the plots of multi-GeV one in Fig. 1(e)–(h) for the large θ_{12} angle solution, $\Delta m^2_{12} = 3\times10^{-5}\mathrm{eV}^2$ and $\sin^2 2\theta = 0.7$. In these figures, broken thick, broken thin and dotted curves denote the regions allowed in 99%, 95% and 90% C.L., respectively. The combinations of the sub-GeV and multi-GeV experiments are shown in Fig. 1 (i)–(l). Fig. 2 represents the case of the small θ_{12} angle solution, $\Delta m^2_{12} = 10^{-5}\mathrm{eV}^2$ and $\sin^2 2\theta = 0.005$.

From these plots, we can get the following results for the mixing parameters:
(1) Δm^2_{23} is allowed from $10^{-2}\mathrm{eV}^2$ to $2\times10^{-4}\mathrm{eV}^2$. The minimum χ^2 is obtained as 14.5 at $\Delta m^2_{23} = 7\times10^{-4}\mathrm{eV}^2$, $\tan^2\theta_{13} = 6\times10^{-2}$ and $\tan^2\theta_{23} = 2$. The minimum χ^2 in the restriction $\theta_{13} = 0$, which corresponds to the $\nu_\mu - \nu_\tau$ mixing, is 17 at $\Delta m^2_{23} = 2\times10^{-3}\mathrm{eV}^2$.

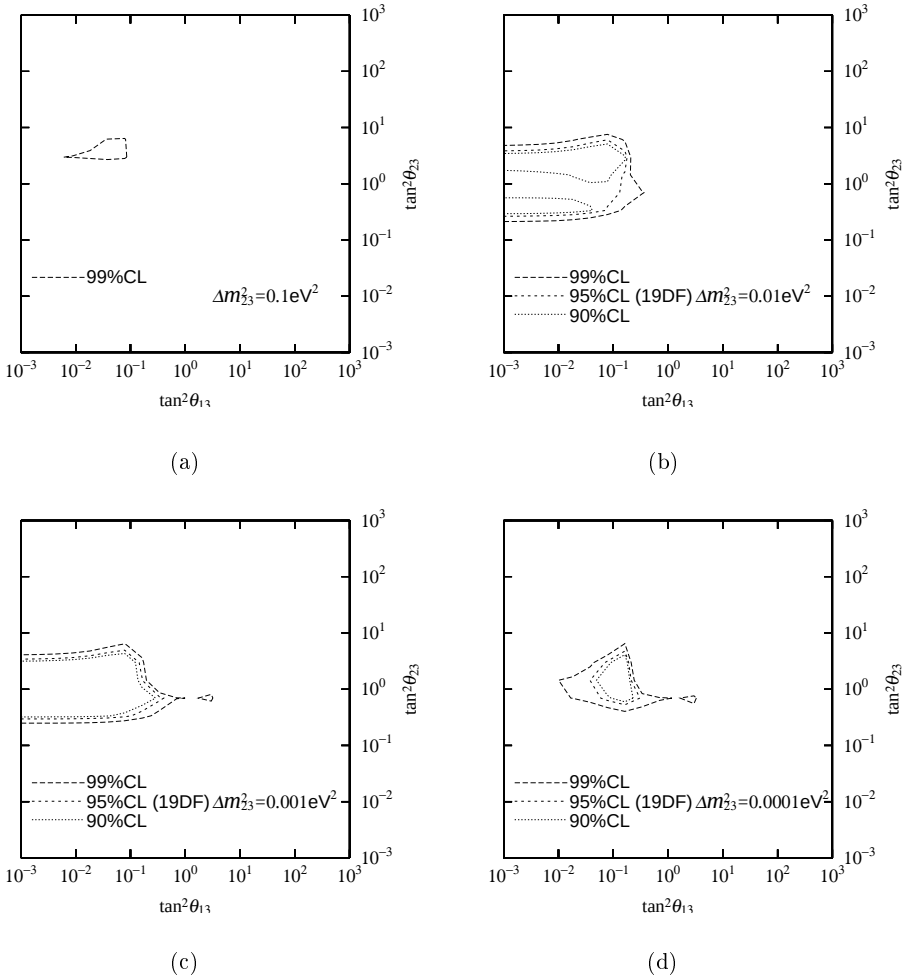

Fig. 2. The plots of allowed regions on $\tan^2\theta_{13}$–$\tan^2\theta_{23}$ plane determined by the zenith angle distributions of the combination of sub-GeV and multi-GeV μ SuperKamiokande 535 days data. These figures correspond to the small θ_{12} angle solution, $\Delta m^2_{12} = 10^{-5}\text{eV}^2$ and $\sin^2 2\theta - 0.005$. In these figures, broken thick, broken thin and dotted curves denote the regions allowed in 99%, 95% and 90% C.L., respectively.

(2) $\nu_e - \nu_\tau$ mixing is small and $\nu_\mu - \nu_\tau$ mixing is large; $\tan^2\theta_{13} < 10^{-1}$ and $\tan^2\theta_{23} \sim 1$.
(3) There is no significant difference between the large θ_{12} solution and small one.
The result that Δm^2_{23} is allowed from 10^{-2}eV^2 to $2\times10^{-4}\text{eV}^2$ and the minimum χ^2 in the restriction $\theta_{13} = 0$ is obtained at $\Delta m^2_{23} = 2\times10^{-3}\text{eV}^2$ is the same as the result obtained by SuperKamiokande collabolation. [1)]

Plots of the upward through-going μ are shown in Fig. 3(a)–(d) and the combinations of the sub-GeV, multi-GeV and upward through-going μ flux in Fig. 3(e)–(h) for the large θ_{12} angle solution. The plots for the small θ_{12} angle solution is the similar to the Fig. 3. From these result, we can say that
(1) the mixing parameters allowed in the sub-GeV and multi-GeV zenith angle distributions can explain the upward through-going μ flux experimental data,

(2) in large value of $\Delta m^2_{23} \sim 10^{-1}$–$10^{-2}\mathrm{eV}^2$, the values near 45° of θ_{23} are excluded, because the deficit from 1 of the event ratio $N_{\mathrm{Exp}}(\mu)/N_{\mathrm{MC}}(\mu)$ is not so large (about 0.2) in upward through-going μ flux compared with multi-GeV experiments.

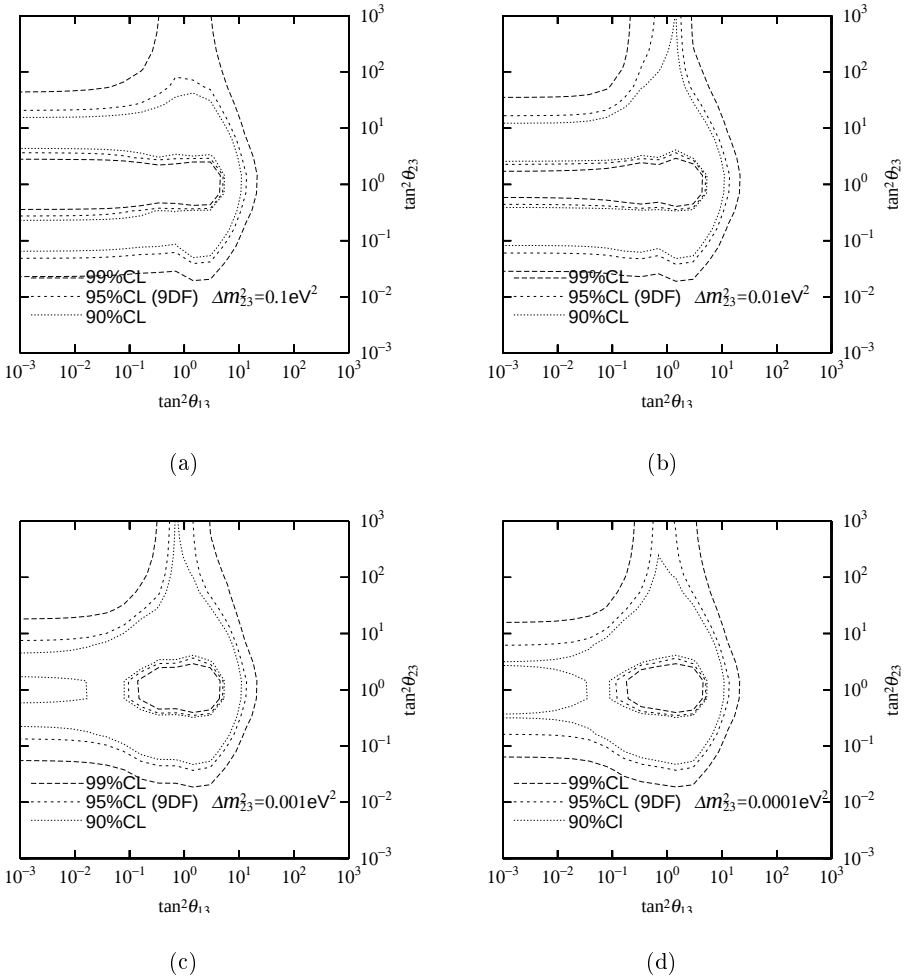

Fig. 3. The plots of allowed regions in the $\tan^2\theta_{13}$–$\tan^2\theta_{23}$ plane determined by the zenith angle distributions of the upward through-going μ SuperKamiokande data for large θ_{12} angle solution. There is no difference between the large θ_{12} angle solution and small one. In these figures, the broken thick, broken thin and dotted curves denote the regions allowed in 99%, 95% and 90% C.L., respectively. Fig. (a)–(d) show the plot of the upward through-going μ experiments.

3.2. *Terrestrial neutrinos*

By many terrestrial experiments, the strong restrictions are imposed to neutrino mixing parameters and masses. In terrestrial experiments, there are two types of experiments, short baseline and long baseline experiments.[8] In this paper, we analyze the short baseline experiments. Accelerator experiments searching for the appearance of ν_τ in ν_μ were performed by

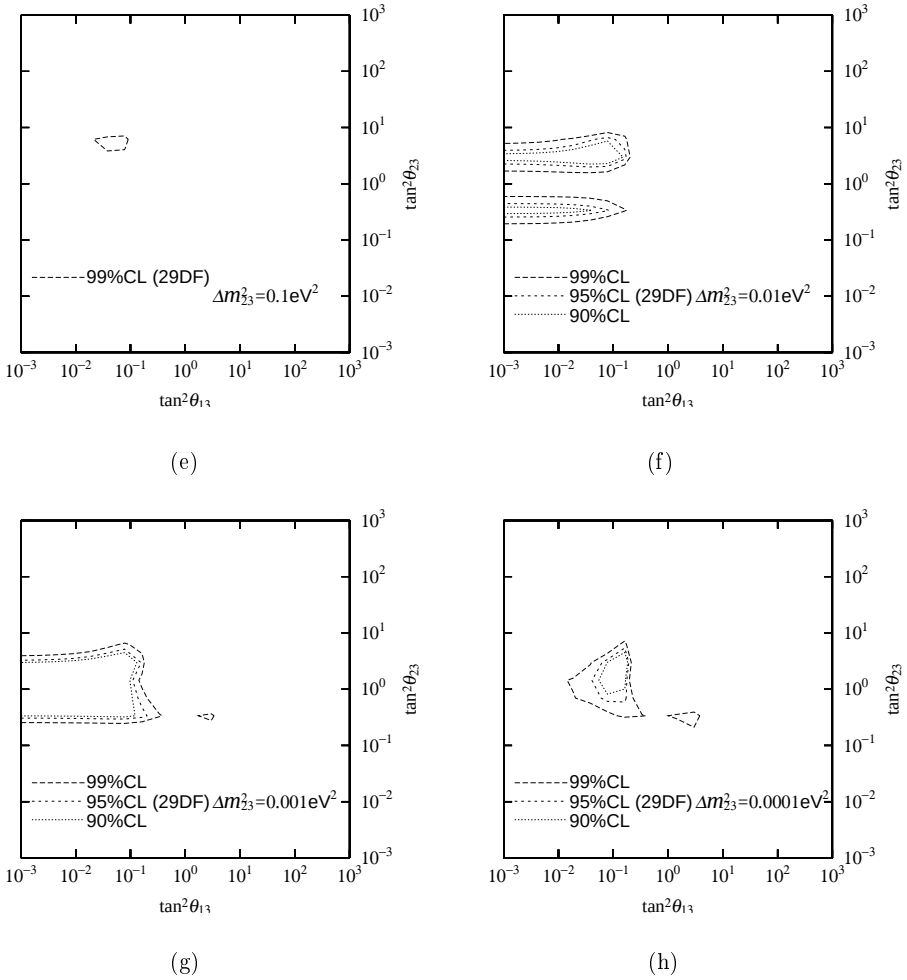

Fig. 3. The plots of allowed regions in the $\tan^2\theta_{13}$–$\tan^2\theta_{23}$ plane for the combinations of sub-GeV, multi-GeV and upward through-going μ experiments.

E531, CHORUS and NOMAD [5)]

$$P(\nu_\mu \to \nu_\tau) < 2 \times 10^{-3} \quad (90\%\ \text{C.L.}), \qquad (12)$$
$$L/E \sim 0.02.$$

Accelerator experiments searching for the $\nu_\mu \to \nu_e$ and $\bar{\nu}_\mu \to \bar{\nu}_e$ oscillations were accomplished by E776, KARMEN and LSND [6)],

$$P(\nu_\mu \to \nu_e) < 1.5 \times 10^{-3} \quad (90\%\ \text{C.L.}), \quad \text{E776} \qquad (13a)$$
$$L = 1\text{km}, \quad E \sim 1\text{GeV},$$
$$P(\bar{\nu}_\mu \to \bar{\nu}_e) < 3.1 \times 10^{-3} \quad (90\%\ \text{C.L.}), \quad \text{KARMEN} \qquad (13b)$$
$$L = 17.5\text{m}, \quad E < 40\text{MeV},$$
$$P(\bar{\nu}_\mu \to \bar{\nu}_e) = 3.4^{+2.0}_{-1.8} \pm 0.7 \times 10^{-3}, \quad \text{LSND} \qquad (13c)$$
$$L = 30\text{m}, \quad E \sim 36 - 60\text{MeV}.$$

Accelerator experiment searching for the disappearance of ν_μ was carried out by CDHSW experiment and the nuclear power reactor experiments searching for the disappearance of $\bar{\nu}_e$ were carried out by the BUGEY experiment and CHOOZ experiment.[7)]

$$\nu_\mu-\text{disappearance experiment, CDHSW} \tag{14a}$$
$$0.26\text{eV}^2 < \Delta m^2 < 90\text{eV}^2 \text{ are excluded for maximal mixing,}$$
$$L = 130,\ 885\text{m}, \quad E \sim 3\text{GeV}.$$
$$1 - P(\bar{\nu}_e \to \bar{\nu}_e) < 10^{-2} \ \ (90\%\ \text{C.L.}), \quad \text{BUGEY} \tag{14b}$$
$$L = 15,\ 40,\ 95\text{m}, \quad E \sim 1 - 6\text{MeV}.$$
$$P(\bar{\nu}_e \to \bar{\nu}_e) = 0.98 \pm 0.04 \pm 0.09, \quad \text{CHOOZ} \tag{14c}$$
$$L = 1\text{km}, \quad E \sim 3\text{MeV}.$$

We show the contour plots of allowed regions in the $\tan^2\theta_{13}$–$\tan^2\theta_{23}$ plane determined by the probability P expressed in Eq. (6) satisfying above experimental data Eqs. (12), (13) (except LSND data (13c)) and (14) in Fig. 4. Allowed regions are left- and right-hand sides surrounded by curves. The curves represent the boundary of 90 % C.L. of P. We fixed the parameters Δm^2_{12} and θ_{12} as $\Delta m^2_{12} = 10^{-5}\text{eV}^2$ and $\sin^2 2\theta_{12} = 0.8$, and the various values of parameter Δm^2_{23} between 0.1eV^2 and $0.0001\ \text{eV}^2$. Although we fix the parameters Δm^2_{12} and θ_{12} as $\Delta m^2_{12} = 10^{-5}\text{eV}^2$ and $\sin^2 2\theta_{12} = 0.01$, the results are not changed, because the probability P of a terrestrial neutrino is insensitive to the $\nu_e - \nu_\mu$ mixing parameters Δm^2_{12} and $\sin^2 2\theta_{12}$. The dotted lines show the allowed regions restricted by LSND data Eq. (13c). The allowed regions determined by LSND data are very restricted, then hereafter we do not consider it.

3.3. *Allowed regions of mixing parameters*

Here, We discuss the allowed regions for mixing parameters Δm^2_{12}, $\sin^2 2\theta_{12}$, Δm^2_{23}, θ_{13} and θ_{23} satisfying atmospheric neutrino and terrestrial neutrino experiments. Δm^2_{12} and $\sin^2 2\theta_{12}$ have been determined in analyses considering the MSW effects of the solar neutrino experiments:[4), 13), 10)]

$$(\Delta m^2_{12},\ \sin^2 2\theta_{12}) = \begin{cases} (4\times10^{-6} - 7\times10^{-5}\text{eV}^2,\ 0.6 - 0.9), & \text{large angle solution} \\ (3\times10^{-6} - 1.2\times10^{-5}\text{eV}^2,\ 0.003 - 0.01). & \text{small angle solution} \end{cases} \tag{15}$$
$$\text{for } \theta_{13} = 0^\circ - 20^\circ$$

Observing the allowed regions obtained in terrestrial neutrino experiments (Fig. 4) and the allowed regions obtained in atmospheric neutrino experiments including sub-GeV and multi-GeV data (Fig. 1 and 2), we obtain the allowed regions consistent with these experi-

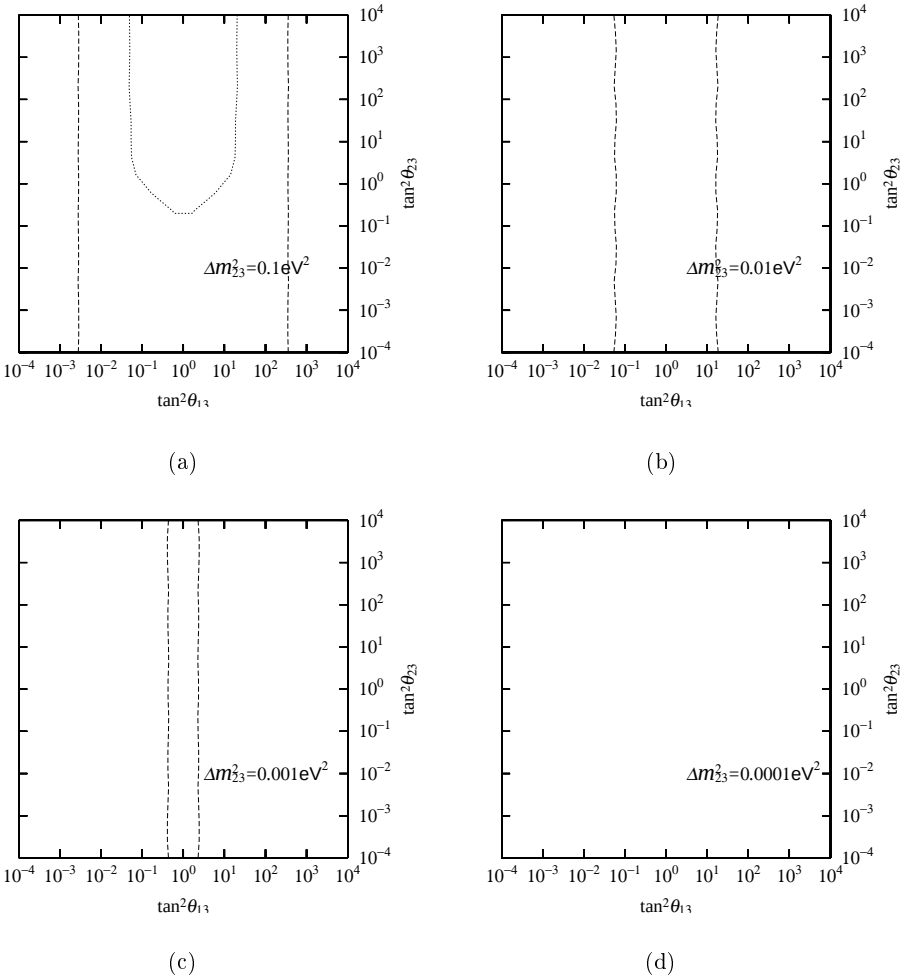

Fig. 4. The plots of allowed regions in the $\tan^2\theta_{13}$–$\tan^2\theta_{23}$ plane determined by P of terrestrial appearance experiments of $\nu_\mu \to \nu_\tau$, $\nu_\mu \to \nu_e$, $\bar{\nu}_\mu \to \bar{\nu}_e$, and the disappearance experiments of $\nu_\mu \to \nu_\mu$ and $\bar{\nu}_e \to \bar{\nu}_e$. The allowed regions are left- and right-hand sides surrounded by curves. The curves represent the boundary of 90 % C.L. of P. Δm^2_{12} and $\sin^2 2\theta_{12}$ are fixed as 10^{-5}eV^2 and 0.8, respectively. Δm^2_{23} is fixed to 0.1eV^2((a)), 0.01eV^2((b)), 0.001eV^2((c)) and 0.0001eV^2((d)). Dotted lines show the allowed regions determined by LSND data.

ments. The allowed regions of θ_{13} and θ_{23} for the large θ_{12} angle solution are as follows:

$$\begin{aligned}
&\text{for } \Delta m^2_{23} = 0.1\text{eV}^2 && \text{no allowed region,}\\
&\text{for } \Delta m^2_{23} = 0.01\text{eV}^2 && (\theta_{13} < 13^\circ,\ 28^\circ < \theta_{23} < 37^\circ,\ 53^\circ < \theta_{23} < 62^\circ),\\
&\text{for } \Delta m^2_{23} = 0.005\text{eV}^2 && (\theta_{13} < 9^\circ,\ 28^\circ < \theta_{23} < 62^\circ),\\
&\text{for } \Delta m^2_{23} = 0.002\text{eV}^2 && (\theta_{13} < 23^\circ,\ 29^\circ < \theta_{23} < 61^\circ),\\
&\text{for } \Delta m^2_{23} = 0.001\text{eV}^2 && (\theta_{13} < 20^\circ,\ 29^\circ < \theta_{23} < 61^\circ),\\
&\text{for } \Delta m^2_{23} = 0.0005\text{eV}^2 && (\theta_{13} < 24^\circ,\ 35^\circ < \theta_{23} < 55^\circ),\\
&\text{for } \Delta m^2_{23} = 0.0002\text{eV}^2 && (4^\circ < \theta_{13} < 22^\circ,\ 38^\circ < \theta_{23} < 54^\circ),\\
&\text{for } \Delta m^2_{23} = 0.0001\text{eV}^2 && \text{no allowed region.}
\end{aligned} \tag{16}$$

For the small θ_{12} angle solution, similar solution is obtained. We cannot see the significant difference between the large θ_{12} angle solution and small one from these results.

If we adopt the 90% C.L. of χ^2 for the zenith angle dependence of atmospheric neutrinos, the range of mass parameter Δm^2_{23} is restricted to as follows;

$$\Delta m^2_{23} = 0.01\text{eV}^2 \sim 0.0002\text{eV}^2. \tag{17a}$$

The value of Δm^2_{23} at the minimum of χ^2 under the constraint of $\theta_{13} = 0$ is obtained near $\tan^2\theta_{23} = 0$ as

$$\Delta m^2_{23} = 2 \times 10^{-3}\text{eV}^2 \ \text{ with } \chi^2 = 17. \tag{17b}$$

Under the no constraint of θ_{13}, the value of Δ^2_{23} at the minimum of χ^2 is obtained at $\tan^2\theta_{13} = 6 \times 10^{-2}$ and $\tan^2\theta_{23} = 2$ as

$$\Delta m^2_{23} = 7 \times 10^{-4}\text{eV}^2 \ \text{ with } \chi^2 = 14.5. \tag{17c}$$

These results (17a) and (17b) are the same as those of SuperKamiokande (Ref. 1) and similar to those of a three-flavor neutrinos analysis (the last paper in Ref. 9)).

The zenith angle distribution of upward through-going μ flux can be explained by the mixing parameter ranges (16) restricted by the zenith angle distributions of sub-GeV and multi-GeV experiments and terrestrial experiments except for the values near 45° of θ_{23} in large value of Δm^2_{23} ($\sim 10^{-1} - 10^{-2}\text{eV}^2$). This exception is because the deficit from 1 of the ratio $N_{\text{Exp}}(\mu)/N_{\text{MC}}(\mu)$ is not so large (about 0.2) in upward through-going μ flux compared with multi-GeV events.

We comment on the present results and ones obtained in our previous analysis.[10] In previous study, we analyzed the double ratios of the zenith angle distributions of atmospheric neutrinos neglecting the matter effects of the Earth and the smearing effects, and obtained the results that the mass of Δm^2_{23} is rather large and the large θ_{12} angle solution is favored than the small one. Analyzing the event ratio in present study, the upper limit of the mass parameter Δm^2_{23} is limited to low value. The difference between large θ_{12} angle solution and small one is disappeared by containing the matter effects of the Earth.

§4. Conclusion

We analyzed the atmospheric neutrino experimental data of SuperKamiokande[1] under the three-flavor neutrino framework with the mass hierarchy $m_1 \approx m_2 \ll m_3$ and obtained the allowed regions of the parameters Δm^2_{12}, $\sin^2 2\theta_{12}$, Δm^2_{23}, θ_{13} and θ_{23}. We studied the event ratios of the sub-GeV, multi-GeV and upward through-going muons zenith angle distributions. From these atmospheric experiments and terrestrial ones, the allowed regions of mass parameters Δm^2_{23} are restricted as 0.01eV^2-0.0002eV^2, and the value of Δm^2_{23} at the minimum χ^2 under the restriction $\theta_{13} = 0$ is $2 \times 10^{-3}\text{eV}^2$. For mixing parameters, there is no difference between the large θ_{12} angle solution and the small θ_{12} one. Obtained results

are $\theta_{13} < 13^\circ$, $28^\circ < \theta_{23} < 37^\circ$ and $53^\circ < \theta_{23} < 62^\circ$ for $\Delta m^2_{23} = 0.01\text{eV}^2$, $\theta_{13} < 23^\circ$ and $29^\circ < \theta_{23} < 61^\circ$ for $\Delta m^2_{23} = 0.002\text{eV}^2$, $\theta_{13} < 24^\circ$ and $35^\circ < \theta_{23} < 55^\circ$ for $\Delta m^2_{23} = 0.0005\text{eV}^2$, $4^\circ < \theta_{13} < 22^\circ$ and $38^\circ < \theta_{23} < 54^\circ$ for $\Delta m^2_{23} = 0.0002\text{eV}^2$. In our three neutrino analysis for the SuperKamiokande atmospheric neutrino experiments, the large $\nu_\mu - \nu_\tau$ mixing is favored and the small mixing $\nu_e - \nu_\mu$ mixing is allowed at the same time. This result will be significant in the long baseline experiments.

Appendix A

—— Explicit calculation of Eqs.(10a) and (10b) ——

In multi-GeV case, the information of the Super-Kamiokande detection efficiency $\epsilon_\alpha(E_\alpha)$ is not known for us, but the detected charged lepton event number $f_\alpha(E_\alpha)$ is given in the paper of SuperKamiokande collaboration.[18] The event number $f_\alpha(E_\alpha)$ is expressed as

$$f_\alpha(E_\alpha) = \int \epsilon_\alpha(E_\alpha)\sigma_\alpha(E_\nu, E_\alpha, \psi)F_\alpha(E_\nu, \theta - \psi)dE_\nu d\cos\psi d\cos\theta. \tag{A·1}$$

We define the effective zenith angle dependent neutrino flux $f_\alpha(E_\alpha, \theta)$ as

$$f_\alpha(E_\alpha, \theta) = f_\alpha(E_\alpha)\frac{F_\alpha(E_\alpha, \theta)}{\int_{-1}^{1} d\cos\theta F_\alpha(E_\alpha, \theta)}, \tag{A·2}$$

where we use the zenith angle distribution given in Ref. 21) for $F_\alpha(E_\alpha, \theta)$. Furthermore we approximate the ψ dependence of differential cross section σ_α by a smearing Gaussian function $n(\psi)$ as

$$n(\psi) = \frac{2}{\sqrt{\pi}\tan(\psi_0/2)}\frac{1}{(1+\cos\psi)\sin\psi}\exp\left\{-\frac{\tan^2(\psi/2)}{\tan^2(\psi_0/2)}\right\}, \tag{A·3}$$

where the resolution ψ_0 is taken as 17°. Then, we estimate $dN_{\text{Exp}}/d\cos\theta$ by the following integral,

$$\frac{dN_{\text{Exp}}}{d\cos\theta} = \int n(\psi)f_\beta(E_\beta, \theta - \psi)P^M(\nu_\beta \to \nu_\alpha)dE_\beta d\cos\psi. \tag{A·4}$$

In sub-GeV case, $\sigma_\alpha(E_\nu) = \int \sigma_\alpha(E_\nu, E_\alpha, \psi)d\cos\psi dE_\alpha$ is calculated in Ref. 24). $\epsilon_\alpha(E_\alpha)$ is nearly 1 in the sub-GeV region, thus we estimate the detected lepton event number with zenith angle dependence $f_\alpha(E_\nu, \theta)$, approximating $\theta = \psi$ in $F_\alpha(E_\nu, \theta - \psi)$,

$$f_\alpha(E_\nu, \theta) = \epsilon_\alpha(E_\nu)\int \sigma_\alpha(E_\nu, E_\alpha, \psi)F_\alpha(E_\nu, \theta)dE_\alpha d\cos\psi = \epsilon_\alpha(E_\nu)\sigma_\alpha(E_\nu)F_\alpha(E_\nu, \theta), \tag{A·5}$$

where information of $F_\alpha(E_\nu, \theta)$ is taken from Ref. 22). Then, introducing the smearing Gaussian function $n(\psi)$ as the multi-GeV case, we express $dN_{\text{Exp}}/d\cos\theta$ as

$$\frac{dN_{\text{Exp}}}{d\cos\theta} = \int n(\psi)f_\beta(E_\nu, \theta - \psi)P^M(\nu_\beta \to \nu_\alpha)dE_\nu d\cos\psi, \tag{A·6}$$

where the resolution ψ_0 is taken as 60° for sub-GeV case.

For upward through-going muons fluxes, event number $f_\alpha(E_\alpha)$ of through-going muons are estimated in Ref. 24). Thus, using this information and the same treatment as multi-GeV case, we calculate the zenith angle θ dependent events of upward through-going muons.

References

[1] Y. Kajita(SuperKamiokande Collaboration), in *Neutrino'98, 18th International Conference on Neutrino Physics and Astrophysics, Takayama, Japan, June 1998*, to appear in the Proceedings.

[2] R. N. Mohapatra and P. B. Pal, *Massive Neutrinos in Physics and Astrophysics* (World Scientific Lecture Note in Physics - Vol.60).

[3] C. Y. Cardall and G. M. Fuller, Phys. Rev. **D 53**(1996), 4421.
G. L. Fogli, E. Lisi, D. Montanio and G. Sciscia, Phys. Rev. **D 56**(1997), 4365.

[4] SAGE Collaboration, J. N. Abdurashitov et al., Phys. Lett. **B328**(1994), 234.
GALLEX Collaboration, P. Anselmann et al., Phys. Lett. **B357**(1995), 237.
B. T. Cleveland et al., Nucl. Phys. **B**(Proc. Suppl.)**38**(1995), 47.
Kamiokande Collaboration, K. S. Hirata *et al.*, Phys. Rev. **D44**, 2241(1991); Phys. Rev. Lett. **66**(1991), 9.
S. A. Bludman, N. Hata, D. C. Kennedy, and P. G. Langacker, Phys. Rev. **D47**, 2220(1993).
N. Hata and P. Langacker, Phys. Rev. **D50**, 632(1994).

[5] E531 Collaboration, N. Ushida et al., Phys. Rev. Lett. **57**(1986), 2897.
K. Winter, Nucl. Phys. **B**(Proc. Suppl.)**38**(1995), 211.

[6] E776 Collaboration, L. Borodovsky et al., Phys. Rev. Lett. **68**(1992), 274.
KARMEN Collaboration, B. Armbruster et al., Nucl. Phys. **B**(Proc. Suppl.)**38**(1995), 235.
LSND Collaboration, C. Athanassopoulos et al., Phys. Rev. Lett. **75**(1995), 2650.
J. E. Hill, Phys. Rev. Lett. **75**(1995), 2654.
W. C. Louis, Nucl. Phys. **B**(Proc. Suppl.)**38**(1995), 229.

[7] F. Dydak et al., Phys. Lett. **B134**(1984), 281.
B. Achkar et al., Nucl. Phys. **B434**(1995), 503.
M. Apollonio et al, Phys. Lett. **B420**(1998), 397.

[8] Y. Oyama(K2K Collaboration), talk at the YITP workshop on flavor physics, Kyoto, Japan, January, 1998. hep-ex/9803014.

[9] G. L. Fogli, E. Lisi and D. Montanino, Phys. Rev. **D52**(1995), 2775.
G. L. Fogli, E. Lisi, D. Montanio and G. Sciscia, Phys. Rev. **D55**(1997), 4385.
C. Giunti, C. W. Kim and M. Monteno, hep-ph/9709439.
G. L. Fogli, E. Lisi, A. Marrone, and G. Sciscia, BARI-TH/309-98, hep-ph/9808205.

[10] T. Teshima, T. Sakai and O. Inagaki, to appear in Int. J. Mod. Phys., hep-ph/9801276.
T. Teshima and T. Sakai, to appear in Prog. Theor. Phys. **101**(1999), No. 1.
[11] Y. Totsuka(SuperKamiokande Collaboration), in *Proceedings of 28th International Symposium on Lepton Photon Interactions, Hamburg, Germany, 1997.*
K. Kaneyuki(SuperKamiokande Collaboration), in *1997 Sectional Meetings of the Physical Society of Japan, Tokyo Metropolitan Univ., Japan, 1997.*
[12] T. Kuo and J. Pantaleone, Rev. Mod. Phys. **61**(1989), 937.
[13] G. L. Fogli, E. Lisi and D. Montanino, Phys. Rev. **D54**(1996), 2048.
[14] P. I. Krastev and S. T. Petcov, Phys. Rev. Lett. **72**(1996), 1960.
[15] G. L. Fogli, E. Lisi and G. Sciscia, Phys. Rev. **D52**(1995), 5334; **D 56**(1997), 3081.
[16] Y. Suzuki, in *Proceedings of 28th International Conference on High Energy Physics, Warsaw, Poland, 1996*, ed. by Z. Ajduk and A. K. Wroblewski (Warsaw University), p.273.
[17] Kamiokande Collaboration, K. S. Hirata et al., Phys. Lett. **B280**(1992), 146.
[18] Kamiokande Collaboration, Y. Fukuda et al., Phys. Lett. **B335**(1994), 237.
[19] IMB Collaboration, R. Becker-Szendy *et al.*, Phys. Rev. **D46**(1992), 3720.
[20] T. K. Gaisser, T. Stanev and G. Barr, Phys. Rev. **D38**(1988), 85.
[21] M. Honda et al., Phys. Rev. **D52**(1995), 4985.
[22] M. Honda et al., private communication.
[23] Vivek Agrawal et al., Phys. Rev. **D53**(1996), 1314.
[24] T. Kajita, *Physics and Astrophysics of Neutrinos*, eds. M. Fukugita and A. Suzuki, (Springer-Verlag, 1994).